FIRST EVIDENCE FOR THE WOBBLING MODE IN A TRIAXIAL SUPERDEFORMED ODD-*A* NUCLEUS*

I. Hamamoto[a], S.W. Ødegård[b,c], G.B. Hagemann[b], D.R. Jensen[b]
M. Bergström[b], B. Herskind[b], G. Sletten[b], S. Törmänen[b]
J.N. Wilson[b], P.O. Tjøm[c], K. Spohr[d], H. Hübel[e], A. Görgen[e]
G. Schönwasser[e], A. Bracco[f], S. Leoni[f], A. Maj[g]
C.M. Petrache[h], P. Bednarczyk[g,i], and D. Curien[i]

[a]Dept. of Mathematical Physics, LTH, University of Lund, Lund, Sweden
[b]The Niels Bohr Institute, Blegdamsvej 17, DK-2100 Copenhagen Ø, Denmark
[c]Dept. of Physics, Univ. of Oslo, PB 1048 Blindern, N-0316 Oslo, Norway
[d]Department of Electronic Engineering and Physics, Univ. of Paisley, Scotland
[e]ISKP, University of Bonn, Nussallee 14-16, D-53115 Bonn, Germany
[f]Dipartemento di Fisica and INFN, Sezione di Milano, Milano, Italy
[g]The H. Niewodniczanski Institute of Nuclear Physics, Kraków, Poland
[h]Dipartemento di Fisica and INFN, Sezione di Padova, Padova, Italy
[i]IReS, 23 rue du Loess, BP28 F-67037, Strasbourg, France

(Received March 30, 2001)

The wobbling mode is uniquely related to rotation of a triaxial body. The Lu–Hf isotopes with $N \sim 94$ provides a possible region of nuclei with pronounced triaxiality. We have investigated ^{163}Lu through the fusion-evaporation reaction ^{139}La(^{29}Si,5n)^{163}Lu with a beam energy of 152 MeV. The electromagnetic properties of several connecting transitions between two presumably Triaxial, SuperDeformed (TSD) bands have been studied. New particle-rotor calculations in which an aligned $i_{13/2}$ proton is coupled to a "wobbling" core are presented and evidence for the assignment of the excited TSD band as a wobbling mode built on the yrast TSD band in ^{163}Lu is given.

PACS numbers: 21.10.–k, 21.10.Re, 23.20.En, 27.70.+q

* Combined contribution from the talks presented by I. Hamamoto and S.W. Ødegård at the *High Spin Physics 2001* NATO Advanced Research Workshop, dedicated to the memory of Zdzisław Szymański, Warsaw, Poland, February 6–10, 2001.

1. Introduction

Rotational bands with the characteristics of SuperDeformed (SD) structures have been observed in several Lu isotopes. In the even N isotopes $^{163-167}$Lu [1–3] the bands are based on the strongly deformation driving proton $i_{13/2}$ configuration, while in odd-odd ^{164}Lu [4], the $i_{13/2}$ proton is coupled to different neutron orbitals. Similar bands have also been observed in even–even ^{168}Hf [5]. At present, the quadrupole moment is only measured in ^{163}Lu ($Q_t \approx 10.7$ b) [1], and ^{168}Hf ($Q_t \approx 11.4$ b) [5]. In all these observed bands, the dynamic moments of inertia are similar and larger than for bands built on Normal Deformed (ND) structures in the same nuclei.

Cranking calculations with the "Ultimate Cranker" [6, 7] predict local minima in the total energy surface for quadrupole deformations of $\varepsilon_2 \sim 0.4$ with a triaxiality of $\gamma \sim \pm 20^\circ$ as a general property for nuclei in the $Z \sim 71$, $N \sim 94$ mass region. Figure 1 shows, as an example, a surface calculated for ^{163}Lu for $I = 53/2$ and $\pi = +$, illustrating the ND minimum together with the local minimum at $\varepsilon_2 \approx 0.4, \gamma \approx +20^\circ$. In general, the local minima with positive value of γ are found at lower energy than the minima with negative

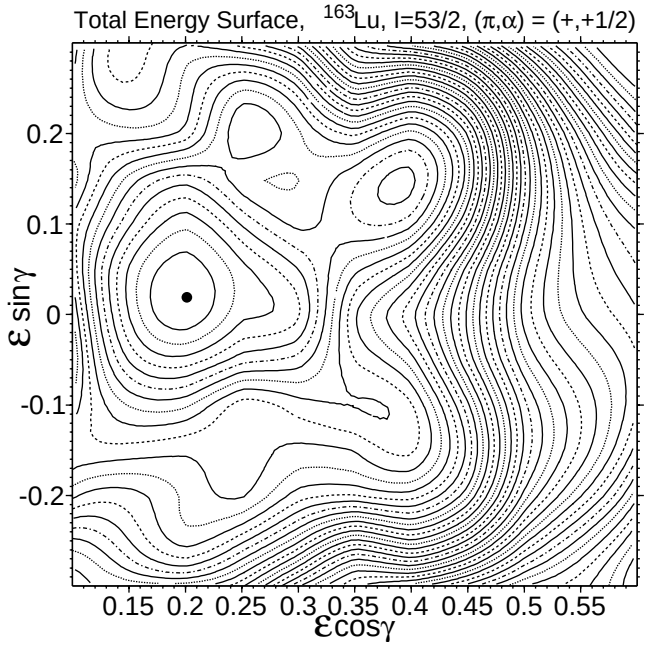

Fig. 1. Total energy surface for ^{163}Lu with $I = 53/2$ and $\pi = +$. The ND minimum together with the local minimum at ($\varepsilon_2 \approx 0.4, \gamma \approx +20^\circ$) are clearly seen while the local minimum at ($\varepsilon_2 \approx 0.4, \gamma \approx -20^\circ$) is rather poorly developed at this spin.

value of γ. The triaxial minima are found for all combinations of parity and signature, and believed to have their origin from a pronounced shell gap at $N = 94$ in the triaxial neutron system.

So far, no direct experimental evidence of the triaxiality of these bands has been found, and the interpretation of these as Triaxial SuperDeformed (TSD) bands has been based on the calculated properties. However, one unique consequence of a rotating nucleus with a triaxial shape would be the existence of "wobbling bands", an excitation mode predicted more than 25 years ago [8], but, until now, never observed in experiment.

For a triaxial body with different moments of inertia with respect to the principal axes, $\mathcal{J}_x \gg \mathcal{J}_y \neq \mathcal{J}_z$, and in the high spin limit with most of the spin aligned along the x axis, the wobbling bands can be represented by a sequence of bands with increasing number of wobbling quanta, $n_{\rm w} = 0, 1, 2, \ldots$. This is illustrated in Fig. 2, where the characteristic pattern of the competition between the in-band transitions and the decay between the bands are indicated. In the present work the detailed properties of the decay transitions between the bands are pinned down from the analysis of experimental data. The comparison between those properties and what is expected from the wobbling mode with aligned particles provides a firm evidence for the wobbling motion in ^{163}Lu.

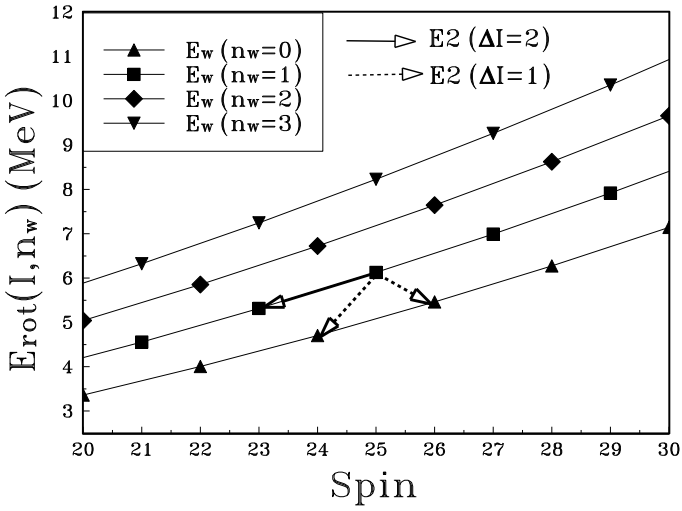

Fig. 2. Wobbling pattern simulated with $\omega_{\rm wob}/\omega_{\rm rot} = 3$.

2. Experimental methods and results

In an early Euroball [9] experiment on ^{163,164}Lu at Legnaro, a second band (TSD2) was observed in ^{163}Lu [10]. This band could not be connected to the rest of the level scheme, although it could be seen in coincidence with TSD1. Carrying about 3 % of the intensity in the channel, as compared to the 10 % of TSD1, this band was considered to be a candidate for a wobbling excitation built on TSD1.

To find the transitions that connect TSD2 to TSD1, a new experiment with the ^{139}La(^{29}Si,5n)^{163}Lu reaction at a beam energy of 152 MeV, was done with the Euroball IV setup [9] at Strasbourg. At the time, 15 Cluster detectors, 25 Clover detectors, and 26 Tapered detectors were used together with the BGO inner ball. With the gating conditions of 3 or more suppressed γ-rays in the Ge detectors and 8 or more γ-rays detected in the BGO inner ball, approximately 2.4×10^9 clean events were collected.

The analysis of the triple coincidences resulted in the partial level scheme presented in Fig. 3, including 9 transitions connecting TSD2 to TSD1. A spectrum of the connecting transitions in coincidence with in-band transitions in TSD1 and TSD2 is displayed in Fig. 4.

To gain further knowledge of the nature of these connecting transitions, the directional correlation of γ-rays from the oriented states (DCO-ratio) was obtained for the strongest transitions using "25°" and "90°" data. In addition, two angular distribution matrices were sorted. The two most forward rings of the Tapered detectors and the most backward ring of the Cluster detectors were included at "25°", while the Clover detectors comprise the "90°" data. Linear polarization measurements were also attempted from two sorted matrices with any angle along one axis and either horizontal or vertical scattering, respectively, within the two rings of Clover detectors, on the other axis. All types of matrices were gated by a list of five clean single gates in TSD1 in any angle in the spin range 21/2–45/2 $\hbar$. The spin alignment, usually parametrised as σ/I for a Gaussian distribution of the m-substate population, $P_m(I) \propto \exp(-\frac{m^2}{2\sigma(I)^2})$ [11], was determined from a comparison of the distribution ratio $W(\text{“25°”})/W(\text{“90°”})$ to the correlation ratio $W(\text{“25°”}\times\text{“25°”})/W(\text{“90°”}\times\text{“25°”})$ in which the experimental detection efficiencies cancel. The comparison was made for a number of stretched electric quadrupole (E2) transitions in the same spin region as the connecting transitions. There was no detectable spin dependence, and an average value of σ/I is 0.25 ± 0.02.

The results of the angular correlation and angular distribution analyses exclude the possibility of pure transitions of stretched dipole or non stretched quadrupole nature. The mixing ratio δ of the electric quadrupole- and magnetic dipole transitions strength E2/M1 has been determined. With no spin

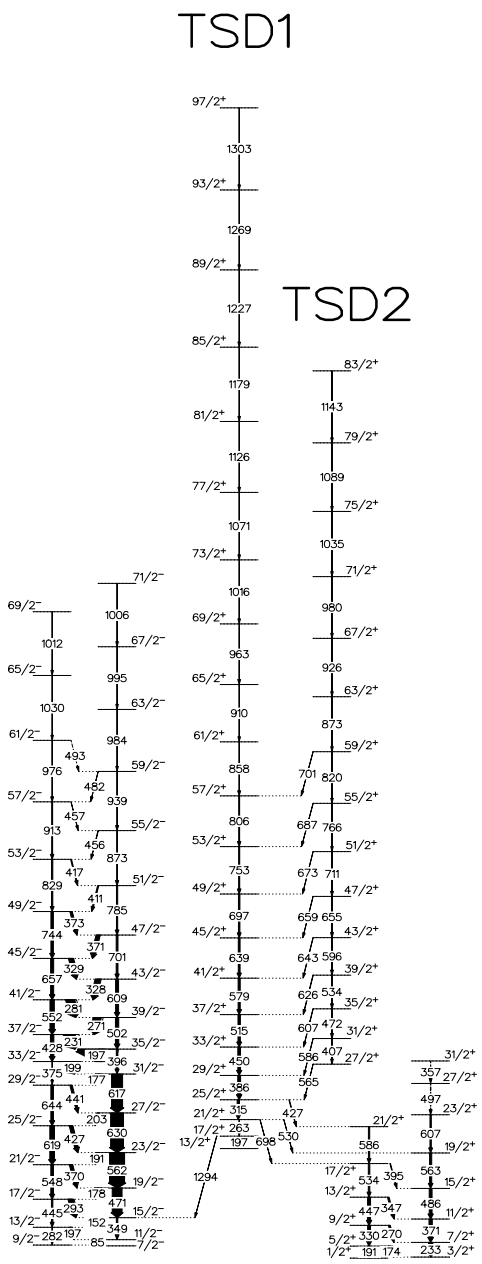

Fig. 3. Partial level scheme of ^{163}Lu showing the two TSD bands together with two of the normal deformed structures in the nucleus.

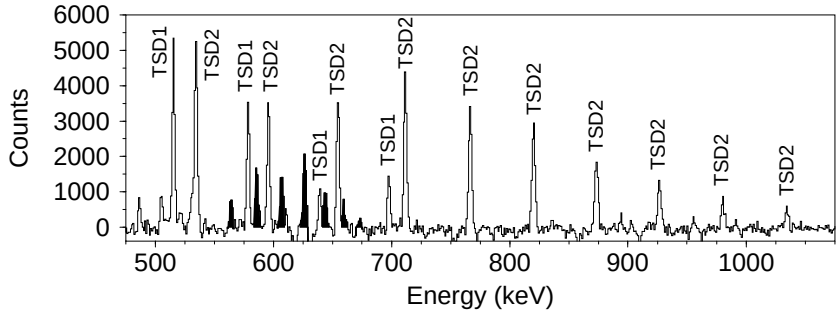

Fig. 4. Sum of double gates:(315+386+450+515+639)⊗(472+595+654+711+766 +820+873+926). Seven of the connecting transitions are marked in black.

dependence within the errors, the extracted values of δ for the different transitions were averaged, and the average values for both methods were combined to give the two possible final values of $\delta = -3.10^{+0.36}_{-0.44}$ or $-0.22^{+0.05}_{-0.03}$. In the polarization measurements the connecting transitions show their electric character, with the same sign and magnitude as the neighbouring stretched E2 in-band transitions, thus excluding the latter solution of $\delta = -0.22^{+0.05}_{-0.03}$.

The final result with $\delta = -3.10^{+0.36}_{-0.44}$ corresponds to $(90.6 \pm 1.3)\,\%$ E2 and $(9.4 \pm 1.3)\,\%$ M1 in the connecting transitions, when disregarding the alternative solution of E1/M2 mixing which would result in unexpectedly large matrix elements for both M2 and E1 transitions.

On the basis of this result the firm parity and signature assignment of TSD2 is $(\pi, \alpha) = (+, -1/2)$, and the excitation energy of TSD2 is only 250–300 keV above TSD1, decreasing as the spin is increasing as illustrated in Fig. 5. The experimental reduced transition probabilities $B(\mathrm{M1})$ and

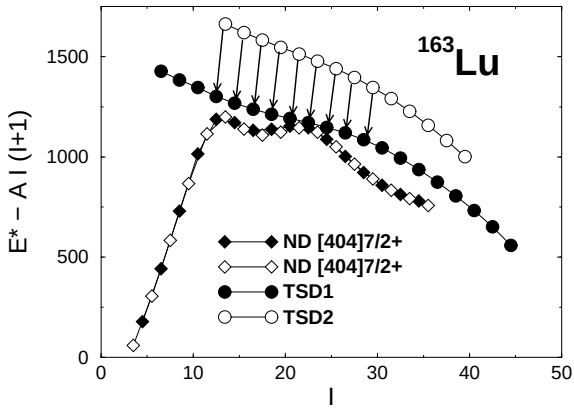

Fig. 5. Level energies of TSD1 and TSD2 together with selected normal deformed levels. A rigid rotor reference has been subtracted.

$B(\mathrm{E2})_{\mathrm{out}}$ can be determined relative to $B(\mathrm{E2})_{\mathrm{in}}$ by the branching ratios $\lambda = T_{\gamma,\mathrm{out}}(\mathrm{M1}+\mathrm{E2})/T_{\gamma,\mathrm{in}}(\mathrm{E2})$ and the mixing ratio $\delta = -3.10^{+0.36}_{-0.44}$ found above. The results for five of the connecting transitions are summarised in Table I. The experimental values are quite similar for all the transitions except for the last one which also has a larger error.

TABLE I

Ratios of reduced electromagnetic moments for the cross-band transitions compared to the in-band transitions in TSD2.

$I(\hbar)$	$E_{\gamma\mathrm{out}}$(keV)	$E_{\gamma\mathrm{in}}$(keV)	$\frac{B(\mathrm{M1})}{B(\mathrm{E2})_{\mathrm{in}}}\left(\frac{\mu_N^2}{e^2b^2}\right)$	$\frac{B(\mathrm{E2})_{\mathrm{out}}}{B(\mathrm{E2})_{\mathrm{in}}}$
35/2	607	472	0.00560 ± 0.00011	0.2125 ± 0.02
39/2	626	534	0.00570 ± 0.00011	0.2020 ± 0.02
43/2	644	595	0.00667 ± 0.00013	0.2238 ± 0.02
47/2	659	654	0.00656 ± 0.00013	0.2102 ± 0.02
51/2	673	711	0.00975 ± 0.00290	0.2994 ± 0.10

3. The wobbling mode with aligned particles

In the wobbling motion of quantum mechanical systems described in the literature the only angular momentum considered in the motion is the total angular momentum I. The wobbling phonon energy is $\hbar\omega_{\mathrm{w}} = \hbar\omega_{\mathrm{rot}} \times \sqrt{(\mathcal{J}_x - \mathcal{J}_y)(\mathcal{J}_x - \mathcal{J}_z)/(\mathcal{J}_y\mathcal{J}_z)}$ with $\hbar\omega_{\mathrm{rot}}{=}I/\mathcal{J}_x$ [12]. In the wobbling motion of nuclei the angular momentum coming from the intrinsic motion can play a role. In the understanding of the experimental data on the SD rotational bands in ^{163}Lu the presence of a high-j aligned particle plays a crucial role in the wobbling motion. The wobbling motion is strongly related to the shell-structure of the nucleus and can appear at relatively low angular momenta. Moreover, the nuclear shell-structure favours a particular (triaxial) shape depending on angular momenta as well as the neutron and proton number.

In the yrast spectroscopy of nuclear high-spin phenomena "high-j" one-particle orbitals have played a special role. The rotational perturbation in the particles occupying those orbitals is so strong that the angular momentum of those particles immediately aligns as rotation sets in. It is known that corresponding to the degree of shell-filling a particular triaxial shape (a particular value of γ) is favoured by the fully aligned high-j particle.

For a single j-shell we can write the triaxially-deformed quadrupole potential in the form

$$V = \frac{\kappa}{j(j+1)}\left(\left(3j_3^2 - j(j+1)\right)\cos\gamma + \sqrt{3}\left(j_2^2 - j_1^2\right)\sin\gamma\right), \qquad (1)$$

where κ, which is proportional to the size of quadrupole deformation β_2, is used as an energy unit [13]. Including the pair correlation with the parameter Δ in the BCS approximation, it is shown [14] that for a given value of $(\lambda, \Delta, \omega)$ the quasiparticle energy is a minimum for $j_x = j$ and the γ-value determined by

$$-2\,\cos(\gamma - 60^\circ) = \frac{\lambda}{\kappa} \qquad \text{for } -2 < \frac{\lambda}{\kappa} < 2\,, \tag{2}$$

where λ expresses the degree of shell-filling while ω denotes rotational frequency. We note that all one-particle energy eigenvalues ε_ν of the potential (1) for a high-j shell lie well inside the region of $-2 < \varepsilon_\nu/\kappa < 2$. Examples given by the relation (2) are:

$$\gamma = \begin{cases} -30^\circ & \text{for} \quad \lambda = 0\,, \\ 0 & \text{for} \quad \frac{\lambda}{\kappa} = -1.0\,, \\ +20^\circ & \text{for} \quad \frac{\lambda}{\kappa} = -1.532\,. \end{cases} \tag{3}$$

The half-filled shell, $\lambda = 0$, corresponds approximately to the case of $h_{11/2}$ protons in β-stable rare-earth nuclei, while (λ/κ)=-1.532 for $\gamma = +20^\circ$ expresses the Fermi level placed just below the lowest one-particle energy eigenvalue. The latter expresses the situation of $i_{13/2}$ protons for the superdeformed bands of ^{163}Lu.

When a given γ value favoured by the aligned particle is supported also by the core, the nucleus may keep the shape in a wide region of angular momentum. In the favoured-signature ($\alpha_{\rm f}$) state with a fully aligned particle the rotation of the core about the axis of the largest moment of inertia for the shape given by Eq. (2) is energetically cheapest. If the triaxial shape is energetically favoured very much by the fully aligned high-j particle, the unfavoured-signature ($\alpha_{\rm u}$) state, which consists of the fully aligned particle together with a wobbling motion of the rotational angular momentum of the core, may appear very low in energy. When the gain in the intrinsic energy of the high-j particle configuration in the wobbling mode wins against the loss in the collective rotation energy of the core, the wobbling mode becomes the lowest $\alpha_{\rm u}$ state. At very high spins the rotational energy dominates over the intrinsic energy and, thus, in the lowest $\alpha_{\rm u}$ state the wobbling mode will be replaced by the cranking-like mode. The possibility of this kind of band crossing of $\alpha_{\rm u}$ states along the yrast lines is pointed out in Ref. [15], taking an example of rotational bands based on $h_{11/2}$ protons in odd-Z β-stable rare-earth nuclei. The unsuccessful attempt of finding such experimental data might be due to the fact that the triaxial shape ($\gamma \approx -30^\circ$) favoured by the aligned $h_{11/2}$ proton was not supported by the core of those odd-Z nuclei in the relevant region of angular momentum.

As described in the introduction, for nuclei with $N \sim 94$ and $Z \sim 71$ the "Ultimate Cranker" [6,7] predicts stable triaxial shapes ($\gamma \sim \pm 20^\circ$) with large quadrupole deformation for all combinations of parity and signature. Following the fact in (3) that $\gamma = +20^\circ$ is preferred by the fully aligned $j = i_{13/2}$ proton in ^{163}Lu, we perform the $i_{13/2}$-particle-rotor calculation along the line of Ref. [15] with parameters $\gamma = +20^\circ$, $\Delta/\kappa = 0.30$, and $\kappa\mathcal{J}_0 = 90$. The latter two parameters are chosen so that the observed level scheme of both TSD1 and TSD2 is, on the average, reproduced using a proper value of κ. Employment of the hydro-dynamical moments of inertia

$$\mathcal{J}_k = \frac{4}{3}\,\mathcal{J}_0 \sin^2\left(\gamma + \frac{2}{3}\pi k\right)\,, \tag{4}$$

where the suffix $k(=1,2,3)$ on the right-hand side should be understood as $k(=x,y,z)$ on the left-hand side, automatically restricts ourselves to the rotation with $-60^\circ < \gamma < 0^\circ$ in the sense of the cranking model. That is, the largest moment of inertia and, consequently, the largest component of collective rotational angular momentum is the one along the intermediate axis of the nuclear shape. In order to get a rotation in the particle-rotor model, which corresponds to $\gamma > 0$ in the cranking sense, we exchange [16] the moments of inertia, $\mathcal{J}_x$ and $\mathcal{J}_y$, obtained from the hydro-dynamical model. For example, $\kappa\mathcal{J}_0$=90 with $\gamma = +20^\circ$ means $\kappa\mathcal{J}_x = 116$, $\kappa\mathcal{J}_y = 50$ and $\kappa\mathcal{J}_z = 14$, so that the system rotates mainly about the x-axis, which is the shortest axis of the $\mid \gamma \mid = 20^\circ$ triaxial shape. If we use the value of $\lambda/\kappa = -1.532$ which is most favourable for the fully aligned $i_{13/2}$ proton at $\gamma = +20^\circ$, the aligned $i_{13/2}$ particle coupled with wobbling motion of the core remains the lowest $\alpha_{\rm u}$ state in the entire region of the total angular momenta of TSD2 discussed in the previous section. We naturally use this value of λ/κ in the calculation of B(M1) and B(E2) values shown in Fig. 6. However, in order to illustrate the band crossing of the "wobbling" regime and the "cranking" regime in the $\alpha_{\rm u}$ states, in Fig. 7 we choose $\lambda/\kappa = -1.20$, for which the "cranking" regime becomes energetically lower than the "wobbling" regime at angular momentum values $\approx 35/2\hbar$, considerably lower than in the case of $\lambda/\kappa = -1.532$.

In Fig. 7 the expectation values of R, R_x and j_x calculated by using the wave functions of the lowest-lying states in the particle-rotor model are shown as a function of the total angular momentum, I,

$$\vec{I} = \vec{R} + \vec{j}\,, \tag{5}$$

where $\vec{R}$ is the rotational angular momentum of the core. In the present model both I and j are good quantum numbers, while R is not. It is seen that for the yrast $\alpha_{\rm u}(=-1/2)$ states, where $I = \alpha \bmod 2$, we have $j_x \approx j$ and

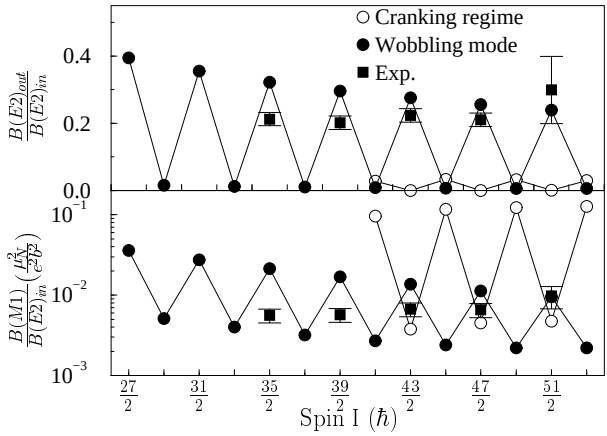

Fig. 6. Experimental and calculated electromagnetic properties of the connecting transitions.

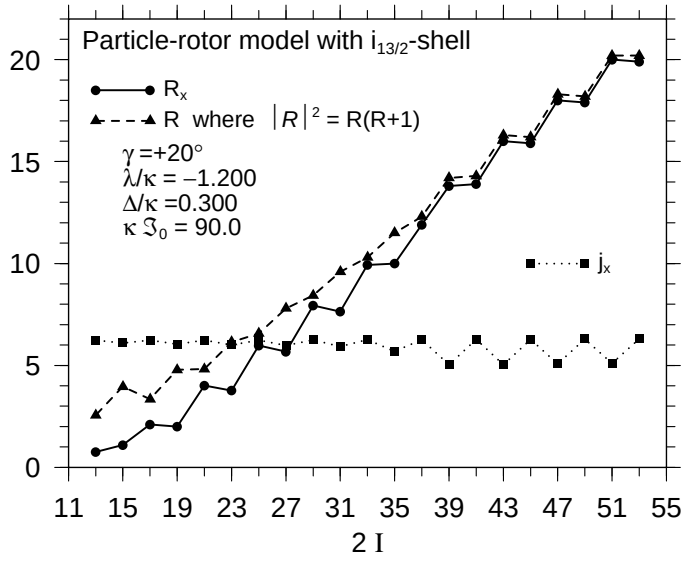

Fig. 7. Expectation values of R, R_x and j_x as a function of the total angular momentum I, which are calculated by using the wave functions of the lowest-lying states in the $i_{13/2}$-particle-rotor model. See the text for details.

$R_x \approx R - 2$ for $I < 35/2$; namely the intrinsic energy with the fully aligned $i_{13/2}$ proton is made to be lowest by the sacrifice of the core rotational energy. On the other hand, for $I > 35/2$ $j_x \approx j - 1$ and $R_x \approx R$; namely the core rotational energy is made to be lowest by the sacrifice of the intrinsic energy. In contrast, for the yrast $\alpha_{\rm f}(= +1/2)$ states we have $j_x \approx j$ and $R_x \approx R$ for all I values, in which both the intrinsic (particle) angular momentum $\vec{j}$

and the core angular momentum $\vec{R}$ can take the respective lowest energy configuration. A proper description is that for $I < 35/2$ the yrast $\alpha_{\rm u}$ states are in the "wobbling" regime, while for $I > 35/2$ they are in the "cranking" regime. Though in the wobbling mode for $\alpha_{\rm u}$ the alignment of the $i_{13/2}$ proton is nearly equal to that of the yrast $\alpha_{\rm f}$ state, the signature splitting of the energy has the same sign as for the signature partner in the cranking mode.

We find that the $\Delta I = 1$ zigzag pattern of both $B({\rm E2})$ and $B({\rm M1})$ values in the "wobbling" regime is out of phase compared with the case of the "cranking" regime. In the "wobbling" regime the $\Delta I = 1$ transition is dominated by $E2$ and not by $M1$. We summarise the characteristic features of the $\Delta I = 1$ electromagnetic transitions between the $\alpha_{\rm u}$ wobbling states and the yrast $\alpha_{\rm f}$ states as follows: (a) $B({\rm M1} : \alpha_{\rm f} I \rightarrow \alpha_{\rm u} I - 1)$ values are reduced, because of $\Delta R_x \approx 2\hbar$; (b) $B({\rm E2} : I \rightarrow I - 1)$ values are of the order of $1/I$ in the limit of high I values, since the wobbling amplitude is of the order of $1/\sqrt{I}$; (c) $B({\rm E2} : \alpha_{\rm f} I \rightarrow \alpha_{\rm u} I - 1)$ values are reduced, because the contributions from Q_0 and Q_2 almost cancel for $\gamma = +20^\circ$. On the other hand, the features of those transitions between the $\alpha_{\rm u}$ states in the "cranking" regime and the yrast $\alpha_{\rm f}$ states may be summarised as: (A) both $B({\rm M1} : \alpha_{\rm u} I + 1 \rightarrow \alpha_{\rm f} I)$ and $B({\rm E2} : \alpha_{\rm u} I + 1 \rightarrow \alpha_{\rm f} I)$ values are reduced, because $\Delta R \approx \Delta R_x \approx 2\hbar$ and, simultaneously $\Delta j_x \approx 1\hbar$; (B) $B({\rm E2} : I \rightarrow I - 1)$ values are small and of the order of $1/I^2$ due to the relevant angular momentum algebra [16]; (C) $B({\rm M1} : \alpha_{\rm f} I \rightarrow \alpha_{\rm u} I - 1)$ values are relatively large being of the order of unity.

4. Comparison to data

In Fig. 6 we show the calculated $B({\rm M1})/B({\rm E2})_{\rm in}$ and $B({\rm E2})_{\rm out}/B({\rm E2})_{\rm in}$ values of the $\Delta I = 1$ transitions between the wobbling $\alpha_{\rm u}$ state and the yrast $\alpha_{\rm f}$ state, in comparison with experimental data on the connecting transitions of mixed E2/M1 nature. We have used the value of $\lambda/\kappa = -1.532$, which is appropriate for the SD bands of ^{163}Lu and, consequently, all calculated $\alpha_{\rm u}$ states are in the wobbling regime. The parameters used in the calculation of $B({\rm M1})$ are $g_s^{\rm eff} = (0.6) g_s^{\rm free}$ and $g_R = 0.4$. For reference, in the figure we also denote $B({\rm M1})$ and $B({\rm E2})$ values in the "cranking" regime, which are calculated using $\lambda/\kappa = -1.20$.

The agreement of the present experimental data with the results calculated for the wobbling mode appears quite satisfactory from Fig. 6 and Table II, in view of the schematic character of the particle-rotor calculations including a single proton $i_{13/2}$ subshell. The failure of a cranking-like solution is particularly obvious from the E2 strength, and the extracted properties summarised in the Table II.

TABLE II

Experimental and calculated values of mixing ratio δ, branching ratio λ and electromagnetic nature of the connecting transition for $I = 43/2\,\hbar \to I = 41/2\,\hbar$. The theoretical values are based on calculated matrix elements and experimental γ-ray energies. For $I = 43/2\,\hbar \to I = 41/2\,\hbar$ in the cranking regime both E2 and M1 transitions are approximately forbidden. Thus, the sign of the mixing ratio can be either plus or minus.

	δ	λ	E/M
exp	$-3.10^{+0.36}_{-0.44}$	0.36 ± 0.04	E
wobbling	-2.4	0.48	E
cranking-like	± 0.15	0.02	M

The observed gradual increase of $B(\mathrm{M1})$ values is not obtained in the present simple model. It may come from the gradual increase of neutron alignment in the core, which is seen in the observed alignment but not included in the calculation of $B(\mathrm{M1})$ values. In the case suggested of TSD2 as a 1-phonon wobbler, the ratio $\hbar\omega_{\mathrm{w}}/\hbar\omega_{\mathrm{rot}}$ varies from 1.5 to 0.5 with increasing spin, indicating a gradual change in the three moments of inertia.

A possible alternative configuration, in which the $\alpha = -1/2$ signature is composed of $\alpha = +1/2$ in the proton system, like TSD1, and a two-quasineutron excitation with $\alpha = 1$, is predicted by UC calculations. This configuration has a local minimum identical to that of TSD1, but the excitation energy is approximately 3–4 times higher than found experimentally for TSD2. Furthermore, an expected additional alignment of $\sim 2\hbar$ relative to TSD1 is not compatible with the data for TSD2. This interpretation is, therefore, disregarded.

5. Summary

The candidate for a wobbling excitation in ^{163}Lu, TSD2, has been connected to TSD1 by 9 linking transitions. The electromagnetic properties together with the alignments are in agreement with the assignment of TSD2 as a wobbling excitation in the presence of an aligned particle, built on TSD1. Alternative interpretations as a signature partner or a three-quasiparticle excitation could be rejected. For the first time, the wobbling mode which uniquely proves the triaxiality of the TSD states is established experimentally.

Fruitful discussions with B. Mottelson and W. Nazarewicz are highly appreciated. This research is supported by the EU TMR project no ERBFMGECT980145, the EU TMR network project, contract no ERBFMRXCT970123, the Danish Science Foundation, the Research Council of Norway, the German BMBF (contract no. 06 BN 907) and the Polish State Committee for Scientific Research (KBN) Grant No. 2 P03B 001 16.

REFERENCES

[1] W. Schmitz, H. Hübel, C.X. Yang, G. Baldsiefen, U. Birkental, G. Fröhlingsdorf, D. Mehta, R. Müsseler, M. Neffgen, P. Willsau, J. Gascon, G.B. Hagemann, A. Maj, D. Müller, J. Nyberg, M. Piiparinen, A. Virtanen, R. Wyss, *Phys. Lett.* **B303**, 230 (1993).

[2] H. Schnack-Petersen, R. Bengtsson, R.A. Bark, P. Bosetti, A. Brockstedt, H. Carlsson, L.P. Ekström, G.B. Hagemann, B. Herskind, F. Ingebretsen, H.J. Jensen, S. Leoni, A. Nordlund, H. Ryde, P.O. Tjøm, C.X. Yang, *Nucl. Phys.* **A594**, 175 (1995).

[3] C.X. Yang, X.G. Wu, H. Zheng, X.A. Liu, Y.S. Chen, C.W. Shen, Y.J. Ma, J.B. Lu, S. Wen, G.S. Li, S.G. Li, G.J. Yuan, P.K. Weng, Y.Z. Liu, *Eur. Phys. J.* **A1**, 237 (1998).

[4] S. Törmänen, S.W. Ødegård, G.B. Hagemann, A. Harsmann, M. Bergström, R.A. Bark, B. Herskind, G. Sletten, P.O. Tjøm, A. Görgen, H. Hübel, B. Aengenvoort, U.J. van Severen, C. Fahlander, D. Napoli, S. Lenzi, C. Petrache, C. Ur, H.J. Jensen, H. Ryde, R. Bengtsson, A. Bracco, S. Frattini, R. Chapman, D.M. Cullen, S.L. King, *Phys. Lett.* **B454**, 8 (1999).

[5] H. Amro, P.G. Varmette, W.C. Ma, B. Herskind, G.B. Hagemann, G. Sletten, R.V.F. Janssens, M. Bergström, A. Bracco, M. Carpenter, J. Domscheit, S. Frattini, D.J. Hartley, H. Hübel, T.L. Khoo, F. Kondev, T. Lauritsen, C.J. Lister, B. Million, S.W. Ødegård, R.B. Piercey, L.L. Riedinger, K.A. Schmidt, S. Siem, I. Wiedenhöver, J.A. Winger, *Phys. Lett.* **B**, in press.

[6] T. Bengtsson, *Nucl. Phys.* **A496**, 56 (1989); **A512**, 124 (1990).

[7] R. Bengtsson, `www.matfys.lth.se/~ragnar/ultimate.html`

[8] Å. Bohr, B.R. Mottelson, *Nuclear Structure*, Vol.II, Chapter 4, Benjamin, Reading, MA, 1975.

[9] J. Simpson, *Z. Phys.* **A358**, 139 (1997).

[10] J. Domscheit, S. Törmänen, B. Aengenvoort, H. Hübel, R.A. Bark, M. Bergström, A. Bracco, R. Chapman, D.M. Cullen, C. Fahlander, S. Frattini, A. Görgen, G.B. Hagemann, A. Harsmann, B. Herskind, H.J. Jensen, S.L. King, S. Lenzi, D. Napoli, S.W. Ødegård, C. Petrache, H. Ryde, U.J. van Severen, G. Sletten, P.O. Tjøm, C. Ur, *Nucl. Phys.* **A660**, 381 (1999).

[11] T. Yamazaki, *Nucl. Data, Sect.* **A3**, 1 (1967).

[12] Å. Bohr, B.R. Mottelson, *Nuclear Structure*, Vol.II, Chapter 6, Benjamin, Reading, MA, 1975.

[13] I. Hamamoto, *Nucl. Phys.* **A271**, 15 (1976).
[14] I. Hamamoto, B. Mottelson, *Phys. Lett.* **B127**, 281 (1983).
[15] I. Hamamoto, *Phys. Lett.* **B193**, 399 (1987).
[16] I. Hamamoto, B. Mottelson, *Phys. Lett.* **B132**, 7 (1983).